

Quantum-classical correspondence of entropy contours in the transition to chaos

Raphael Zarum and Sarben Sarkar

Department of Physics, King's College London, Strand, London WC2R 2LS, UK

(October 5, 2018)

Von Neumann entropy production rates of the quantised kicked rotor interacting with an environment are calculated. A significant correspondence is found between the entropy contours of the classical and quantised systems. This is a quantitative tool for describing quantum-classical correspondence in the transition to chaos.

I. INTRODUCTION

The fundamental split between integrable and non-integrable systems in classical mechanics has not been comprehensively mirrored in quantum mechanics [1]. The issue seems to hinge on finding a suitable definition for *quantum* chaos. The sensitive dependence to initial conditions that characterises classical chaos is wholly understood in terms of trajectories of classical phase space points which have no direct quantum analog [2]. This has led to two distinct ways of identifying variables to measure quantum chaos. One involves investigating various quantum variables that can act as signatures of chaos by clearly distinguishing between quantum systems whose classical counterparts are integrable and those which are non-integrable. The implementation of an expanding array of energy spectra properties have made this approach highly successful (e.g. [3–7]). A second approach seeks an intrinsically quantum definition of quantum chaos by investigating the quantum parallels for variables such as Lyapunov exponents and various entropy measures which define and quantify chaos in classical mechanics [1,2,8–11].

In this paper we adopt the second approach and develop an original technique involving the analysis of entropy production measures to reveal a clear correspondence between the quantum and classical formulations of a seminal system which has a rich structure of delicately interwoven regular and chaotic dynamics - the standard map. Section II A briefly outlines the main characteristics of the standard map and then Section II B describes how classical entropy contours are calculated and used to give a comprehensive account of these characteristics. In a similar fashion, Section III A briefly outlines the quantisation of the standard map and then Section III B describes how quantum entropy contours are generated through interaction with an environment. The similarities and differences between the classical and quantum entropy contours are explained in Section IV A and Section IV B concludes the paper with a discussion on the use of entropy measures to describe quantum chaos.

II. CLASSICAL STANDARD MAP

A. Phase space description

The standard map describes the local behaviour of nonintegrable dynamical systems in the separatrix region of non-linear resonances. The name results from its extensive use in the investigation of chaos, especially the mechanisms involved in the transition to global chaos in conservative systems. It is derived from the kicked rotor model of a one dimensional pendulum and is a Hamiltonian (area preserving) dynamical system. Though the map has been extensively analysed [12–15], here we describe some relevant details.

The standard map can be represented by the equations of motion:

$$\begin{aligned} p_{n+1} &= p_n - \frac{K}{2\pi} \sin(2\pi q_n) \\ q_{n+1} &= q_n + p_{n+1} \pmod{q=1}, \end{aligned} \quad (1)$$

where K is a real variable which acts as the chaos parameter. With unit mass and discrete time, p and q have the same dimensions. The phase space of the map is periodic in q , by definition, and as a special feature of the standard map it is also periodic in p , with the same period 1. $K = 0$ is the case for a free rotor, a trivial and completely regular map. In Fig.1(a)-(c), we show the well known sequence of standard map plots for increasing values of K . The map has several axes of symmetry and the unit periodicity in both p and q means that only a unit square in phase space need be viewed. The interval $[-\frac{1}{2}, \frac{1}{2}]$ is used for all results in this paper. Fig.1(a) shows the mapping when $K = 0.2$. Much of the phase space is composed of KAM (Kolmogorov-Arnold-Moser) tori [3] stretching horizontally from $q = -\frac{1}{2}$ to $q = \frac{1}{2}$ and serve to isolate one region of phase space from another. Periodic orbits in the central resonance can be easily seen, as well as a few other dominant non-linear resonances (small ellipses) between KAM tori.

As K is increased, KAM tori that horizontally span the phase space are destroyed by resonances and are replaced with smaller KAM islands. Beyond a critical value at $K \approx 0.97$, the last phase space spanning KAM torus is broken and the map becomes globally chaotic (Fig.1(b)).

Now the remaining resonances are clearly visible as *stable islands* in a *chaotic sea* of trajectories. On reaching $K = 4$, most structure is wiped out (Fig.1(c)).

B. KS entropy contours

A positive Lyapunov exponent, which quantifies the exponential divergence in time of two closely neighbouring phase space trajectories, is a primary definition of classical chaos [16]. For one-dimensional maps such as the standard map the positive Lyapunov exponent is equal to the Kolmogorov-Sinai (KS) entropy, h_{KS} , which is a measure of the rate of information production in the system [17,18]. Thus $h_{KS} = 0$ only for completely regular dynamics. The KS entropy (also called dynamical entropy or metric entropy) of a chaotic mapping can be calculated using the formula

$$h_{KS} = \lim_{t \rightarrow \infty} \left(\frac{1}{t} \right) \sum_{n=1}^t \log_2 l_n, \quad (2)$$

where $l_n = \sqrt{(\delta p_n)^2 + (\delta q_n)^2}$ is the changing distance between two initially close neighbouring points, (p_0, q_0) and $(p_0 + \delta p_0, q_0 + \delta q_0)$, in phase space. δp and δq are evolved by iterating a linearised form of the chaotic map. This *tangent map* is rescaled after every iteration as follows: the n^{th} iteration of the map produces the values δp_n and δq_n from which l_n is calculated. These values are then rescaled to $\delta \bar{p}_n = \delta p_n / l_n$ and $\delta \bar{q}_n = \delta q_n / l_n$ which are fed back into the tangent map for the next iteration [12]. Use of the base-2 logarithm in (2) allows the entropy to be measured in *bits* of information.

The standard map is linearised to give its associate tangent map

$$\begin{pmatrix} \delta p_{n+1} \\ \delta q_{n+1} \end{pmatrix} = \begin{pmatrix} 1 & K \cos(2\pi q_n) \\ 1 & 1 + K \cos(2\pi q_n) \end{pmatrix} \begin{pmatrix} \delta p_n \\ \delta q_n \end{pmatrix}, \quad (3)$$

which can be employed in (2) to calculate h_{KS} .

The tangent map (3) clearly shows that the value of h_{KS} depends on the initial position in phase space (p_0, q_0) for the standard map. This is not always the case. h_{KS} is generally used as a *global* measure of the level of chaos in a given system, but this is only valuable if all chaotic trajectories in the system can reach into all regions of its phase space. Well known examples of such systems include the cat and baker's maps [19]. However for $K < 1$ the standard map has a predominantly *mixed* phase space in which different chaotic regions are not connected. KAM tori act as boundaries so that trajectories originating in one chaotic region cannot escape to another. This isolation inhibits the exponential divergence of chaotic trajectories so that the positive Lyapunov exponent, and consequently h_{KS} , will vary from region to region. The kicked top is another example of a well known mixed phase space system [20].

To reveal a *complete* description of the standard map at a specific K in terms of KS entropy, many values of h_{KS} corresponding to many initial positions in phase space can be plotted as a contour map on phase space. This has been done in Fig.1(d)-(f). Using (2) and (3), and setting $t = 10^5$ iterations, values for h_{KS} were calculated for each point on a 64×64 grid spanning the same unit of phase space and the same K values as in Fig.1(a)-(c). Shading intensity reflects the relative sizes of the KS entropy. $h_{KS} = 0$ is shown as white on the maps while darker and darker shades of grey reflect an increasing h_{KS} . The black areas show the largest h_{KS} values corresponding to the most chaotic regions of the standard map. The resemblance between Fig.1(a)-(c) and Fig.1(d)-(f) is striking. Stable islands in the classical maps translate to stark white patches in the contour maps. This is because $h_{KS} = 0$ for *all* periods in non-chaotic dynamics. The chaotic sea of trajectories in the classical maps are also faithfully reproduced as very dark patches of similar shape and size in the contour maps. All these correlations indicate that h_{KS} presented in this way can comprehensively display all the essential features of the standard map as it becomes globally chaotic.

III. QUANTUM KICKED ROTOR

A. Quantization

The quantised model of the standard map is governed by the Hamiltonian

$$\hat{H}_{stan}(\hat{p}, \hat{q}, t) = \frac{\hat{p}^2}{2} - \frac{K}{4\pi^2} \cos(2\pi \hat{q}) \sum_{n=-\infty}^{\infty} \delta(t - nT). \quad (4)$$

This “kicked rotor” describes a free particle of unit mass which experiences impulses (kicks) at intervals T . Following [21] and [22], the kinematics are that of finite dimensional quantum mechanics with periodic boundary conditions. Position and momentum space are thus discretized, placing the lattice sites at integer values $q_a = p_a = \frac{a}{D}$ for $a = -\frac{D}{2}, \dots, \frac{D}{2} - 1$. The dimension D of Hilbert space is taken as even and, for consistency of units, the quantum scale on phase space is taken to be $2\pi\hbar = \frac{1}{D}$. Position and momentum basis kets are denoted by $|q_a\rangle$ and $|p_a\rangle$.

Initial states $|\psi_0\rangle$ are assumed to be *coherent states* (minimum-uncertainty states). The fiducial initial coherent state $|\psi_{0\{00\}}\rangle = |q_0, p_0\rangle$ is defined as the ground state of a special Harper operator [23], which can be displaced with the appropriate operators to produce all the other possible initial coherent states $|\psi_{0\{ab\}}\rangle = |q_a, p_b\rangle$, i.e.,

$$|\psi_{0\{ab\}}\rangle = \exp\left(\frac{i\pi ab}{D}\right) \exp(-2\pi i a \hat{p}) \exp(2\pi i b \hat{q}) |\psi_{0\{00\}}\rangle \quad (5)$$

At time t , the system can be described by the density operator $\rho(t) = |\psi(t)\rangle\langle\psi(t)|$ which changes according to the evolution equation

$$\rho(t+T) = \hat{U}_s \rho(t) \hat{U}_s^{-1}, \quad (6)$$

where the kicked rotor unitary evolution operator,

$$\hat{U}_s = \exp\left(\frac{-i\hat{p}^2 T}{2\hbar}\right) \exp\left(\frac{iKT \cos(2\pi\hat{q})}{4\pi^2\hbar}\right). \quad (7)$$

B. Von Neumann entropy contours

Parallelling the classical case, we look for an entropy measure to reveal the dynamics of the quantum system. Entropy in quantum statistical mechanics is referred to as von Neumann (vN) entropy, h_{vN} , (the equivalent measure in classical mechanics is the Gibbs entropy) and can be defined in terms of the density matrix ρ of a system as

$$h_{vN} = -\text{Tr}(\rho \log_2 \rho). \quad (8)$$

h_{vN} is a quantitative measure of disorder and can be measured in bits. However, the unitarity of Hamiltonian dynamical evolution dictates that h_{vN} remain constant at all times. The situation can be altered by perturbing the system through the interaction with an environment. Averaging over the various possible effects of this environment will then lead to an entropy increase Δh_{vN} which can then be employed to measure the system's chaotic nature. This is more than a convenient mathematical construction. To produce a quantum kicked rotor in an experimental situation, the free particle motion must be periodically opened up to an environment to allow the “kick” to be introduced [24]. (Though (6) defines the evolution operator for free motion experiencing an *instantaneous* periodic kick, it is equally valid, as long as the free motion is not concurrent [7], for a *finite* time periodic kick which is what is required to realise this experimentally.) In doing this the environment itself effects the system which naturally causes the entropy increase required.

Thus we choose the environmental coupling to mirror the form of the kick in (4) viz. the q dependence and interaction time. We also choose the environment model to be a collection of degenerate two-state atoms with a range of interaction strengths governed by a normal distribution (this is a generalisation of the class of environments considered by Schack and Caves [9]), so that

$$\hat{H}_{int} = \frac{\alpha \cos(2\pi\hat{q})}{4\pi^2} \otimes \sum_{n=-\infty}^{\infty} \hat{\sigma}_z(n) \delta(t - nT). \quad (9)$$

Thus during the n th kick the rotor interacts with a single two state system with Pauli operator $\hat{\sigma}_z(n)$ and

interaction strength α . Each of the two-state environment systems is equally likely to be in the “up” state $|\uparrow\rangle$, where $\hat{\sigma}_z|\uparrow\rangle = |\uparrow\rangle$, or in the “down” state $|\downarrow\rangle$, where $\hat{\sigma}_z|\downarrow\rangle = -|\downarrow\rangle$. Also, α is drawn from a collection of $M+1$ independent interaction strengths such that $\alpha = \alpha_j$ for $j = -\frac{M}{2}, \dots, 0, \dots, \frac{M}{2}$. The distribution P_{α_j} for α_j is the normal distribution $N(\alpha_0, \alpha_{sd}^2)$.

The combined Hamiltonian for the coupled system and environment is thus

$$\hat{H}_{tot} = \hat{H}_{stan} + \hat{H}_{int}, \quad (10)$$

and the corresponding density operator evolution equation is

$$\rho(t+T) = \hat{U}_{tot}(\alpha, \lambda) \rho(t) \hat{U}_{tot}^{-1}(\alpha, \lambda), \quad (11)$$

where the combined evolution operator,

$$\hat{U}_{tot}(\alpha, \lambda) = \exp\left(\frac{-i\alpha\lambda T \cos(2\pi\hat{q})}{4\pi^2\hbar}\right) \hat{U}_s, \quad (12)$$

with $\lambda \in \{-1, 1\}$ is the result of measuring the two state environment after each interval to determine whether it is an up or down state. (As before, this same operator would result if (9) was turned on for the *finite* time required for an experimental realisation of this system.) The effect of this environmental coupling is to produce a multiple stochastic perturbation at the end of each time interval. After each interval, there are $2M+2$ different measurement results leading to $2M+2$ possible pure states for the system. Averaging over all these possible outcomes in the position basis produces the density operator evolution equation

$$\begin{aligned} \bar{\rho}_{xy}(t+T) &\equiv \langle x | \bar{\rho}(t+T) | y \rangle \\ &= \sum_{j=1}^{M+1} \frac{P_{\alpha_j}}{2} \sum_{\lambda=-1,1} \langle x | \hat{U}_{tot}(\alpha_j, \lambda) \bar{\rho}(t) \hat{U}_{tot}^{-1}(\alpha_j, \lambda) | y \rangle \\ &= F(x, y) \langle x | \hat{U}_s \bar{\rho}(t) \hat{U}_s^{-1} | y \rangle, \end{aligned} \quad (13)$$

where

$$F(x, y) = \sum_{j=1}^{M+1} P_{\alpha_j} \cos\left(2\alpha_j D \pi \sin \frac{\pi(x+y)}{D} \sin \frac{\pi(x-y)}{D}\right) \quad (14)$$

now contains all the perturbation effects due to the environment. This causes a vN entropy increase which can be determined by tracing over the system so that,

$$\Delta h_{vN}(nT) = -\text{Tr}(\bar{\rho}(nT) \log_2 \bar{\rho}(nT)), \quad (15)$$

where $\bar{\rho}(nT)$ is the average density matrix of the system after n time intervals.

One final step will allow us to see the quantum chaotic dynamics. Zurek and Paz [10] have conjectured that for an *open* quantum system with minimal dissipation which

displays classical chaos, the *rate* of vN entropy production, \tilde{h}_{vN} , of its quantum analogue, after an initial decoherence time, t_d , will rise to a maximum value which is solely dependent on the sum of its positive Lyapunov exponents. This will continue to be the case until the system begins to approach equilibrium when \tilde{h}_{vN} will slowly decrease reaching zero at time t_{eqm} . In contrast, the entropy production rate of the quantum analogue of a regular systems will asymptotically tend to zero well before t_{eqm} . Applying this to the standard map, \tilde{h}_{vN} for the quantised system interacting with an environment should be comparable to the KS entropy of its classical (unperturbed) counterpart. Thus for $t_d < nT \ll t_{eqm}$,

$$\tilde{h}_{vN} \approx \frac{\Delta h_{vN}(nT) - \Delta h_{vN}((n-1)T)}{T} \approx h_{KS}. \quad (16)$$

A uniformly spaced 64 x 64 grid of initial coherent states (corresponding to an even spread over unit phase space) were numerically evolved in time. The maximum value of \tilde{h}_{vN} for each evolution was plotted on a contour map in a similar fashion to the classical case. Fig.1(g)-(i) displays the results for the same three values of K with $D = 256$, $\alpha_0 = 0.001$, $\alpha_{sd} = 0.2\alpha_0$, $M = 100$ and $T = 1$.

IV. DISCUSSION

A. Quantum-classical correspondence

There are remarkable similarities between Fig.1(d)-(f) and Fig.1(g)-(i). For the same K values, the size and location of the various stable islands is analogous, dark patches are prevalent in the heavily chaotic regions, the axes of symmetry are consistent and the overall complexity of the dynamics is clearly visible in both.

There are also differences. The quantum contour maps are generally much smoother than their classical counterparts. This is because each initial coherent state in the quantum system has a support area causing their evolution to imitate that of a *density* of points on phase space. Thus neighbouring coherent states will fail to achieve dramatically different rates of vN entropy production. Increasing D reduces the supports of the initial coherent states as well as reducing the overlap between neighbouring states. It was found that this led to a reduction in the smoothness of the quantum contour maps making them more greatly resemble the classical contour maps.

The process of calculating these entropy contour maps was repeated with variations to $N(\alpha_0, \alpha_{var}^2)$. For $\alpha_0, \alpha_{sd} \ll K$, when any entropy increase is due primarily to the chaotic dynamics of the system and not the interaction, similar results were achieved.

B. Conclusion

We have demonstrated that an entropy based approach allows classical chaotic dynamics to be accurately measured in a trajectory independent way which in turn makes it eminently suitable to measure [25] and analyse the corresponding quantum chaotic dynamics. We have also given numerical support to the Zurek and Paz conjecture in a chaotic system which folds phase space, a characteristic that their conjecture did not directly take into account.

Entropy measures for diagnosing chaotic dynamics can also be employed in other maps. The sawtooth map [26] (which becomes Arnold's cat map [19] for a specific value of the chaos parameter K) does not have a mixed phase space so entropy contours would be of little interest. However, correspondence *can* be investigated by comparing quantum and classical entropy measures for a *range* of K values. Even more interesting is the kicked top [20] which is described by a map on the unit sphere. Like the standard map, it has a predominantly mixed phase space for lower values of its chaos parameter making it ideal for comparing classical and quantum entropy contours. The kicked top also has a special "order-within-chaos" [27] feature. In general h_{KS} increases monotonically with the chaos parameter K of a given map. However, the kicked top has islands of stability reappearing for specific higher K values when the map is already globally chaotic. This leads to an intricate relationship between h_{KS} and K which can be compared to numerical results for the corresponding \tilde{h}_{vN} . We will discuss the results for these maps elsewhere.

Finally, KS entropy is information-theoretically defined as the rate of production of Shannon entropy (also called the Shannon information measure) [28]. Thus, within well defined parameters, we have shown that the quantum-classical correspondence of chaotic dynamical systems may be realised by viewing the Shannon entropy production rate as the classical measure corresponding to the quantum measure of the von Neumann entropy production rate. These results provide a new diagnostic for investigating the chaotic nature of quantum systems.

ACKNOWLEDGEMENTS

We are grateful to the ESPRC for their financial support. RZ would like to thank Rüdiger Schack for useful discussions.

-
- [1] J. Ford, G. Mantica and G.H. Ristow, Physica D **50**, 493 (1991).
 - [2] R. Schack and C.M. Caves, Phys. Rev. E **53**, 3387 (1996).

- [3] L.E. Reichl, *The Transition to Chaos in Conservative Classical Systems: Quantum Manifestations* (Springer-Verlag, Berlin, 1992).
- [4] M.V. Berry, in *Chaotic Behaviour in Deterministic Systems, Les Houches XXXVI*, edited by G. Iooss, R.H.G. Hellman and R. Stora (North-Holland Amsterdam, 1991).
- [5] F. Haake, *Quantum Signatures of Chaos*, (Springer-Verlag, Berlin, 1991).
- [6] M.C. Gutzwiller, *Chaos in Classical and Quantum Mechanics* (Springer-Verlag, New York, 1990).
- [7] M. Tabor, *Chaos and Integrability in Nonlinear Dynamics: An Introduction*, (Wiley, New York, 1989).
- [8] W. Ślomyński and K. Życzkowski, J. Math. Phys. **35**, 5674 (1994); S. Klimek and A. Leśniewski, Ann. Phys. (N.Y.) **248**, 173 (1996).
- [9] R. Schack and C.M. Caves, Phys. Rev. E **53**, 3257 (1996).
- [10] W.H. Zurek and J.P. Paz, Phys. Rev. Lett. **72**, 2508 (1994).
- [11] W.H. Zurek and J.P. Paz, Physica D **83**, 300 (1995).
- [12] B.V. Chirikov, Phys. Rep. **52**, 263 (1979).
- [13] J.M. Greene, J. Math. Phys. **9**, 760 (1968).
- [14] J.M. Greene, J. Math. Phys. **20**, 1183 (1979).
- [15] J.D. Meiss, Rev. Mod. Phys. **63** 795 (1992).
- [16] V.I. Oseledec, Trans. Mosc. Math. Soc. **19**, 197 (1968); J.P. Eckmann and D. Ruelle, Rev. Mod. Phys. **57**, 617 (1985).
- [17] Ya. B. Pesin, Russ. Math. Surveys **32**, 55 (1977).
- [18] G. Benettin, L. Galgani and J.M. Strelcyn, Phys. Rev. A **14**, 2338 (1976).
- [19] V.I. Arnold and A. Avez, *Ergodic Problems of Classical Mechanics* (Benjamin, New York, 1968).
- [20] F. Haake, M. Kuś and R. Scharf, Z. Phys. B **65**, 381 (1987).
- [21] G. Casati, B.V. Chirikov, F.M. Izraelev and J. Ford, in *Lecture Notes in Physics; 93*, edited by G. Casati and J. Ford (Springer-Verlag, 1979).
- [22] M.V. Berry, N.L. Balaszs, M. Tabor and A. Voros, Ann. Phys. (N.Y.) **122**, 26 (1979).
- [23] M. Saraceno, Ann. Phys. (N.Y.) **199**, 37 (1990).
- [24] F.L. Moore, J.C. Robinson, C.F. Bharucha, B. Sundaram and M.G. Raizen, Phys. Rev. Lett. **75**, 4598 (1995).
- [25] S. Sarkar and J.S. Satchell, Physica D **29**, 343 (1988).
- [26] I.C. Percival and F. Vivaldi, Physica D **27**, 373 (1987).
- [27] V. Constantoudis and N. Theodorakopoulos, Phys. Rev. E **56**, 5189 (1997).
- [28] C.E. Shannon and W. Weaver, *The Mathematical Theory of Communication* (University of Illinois Press, 1949).

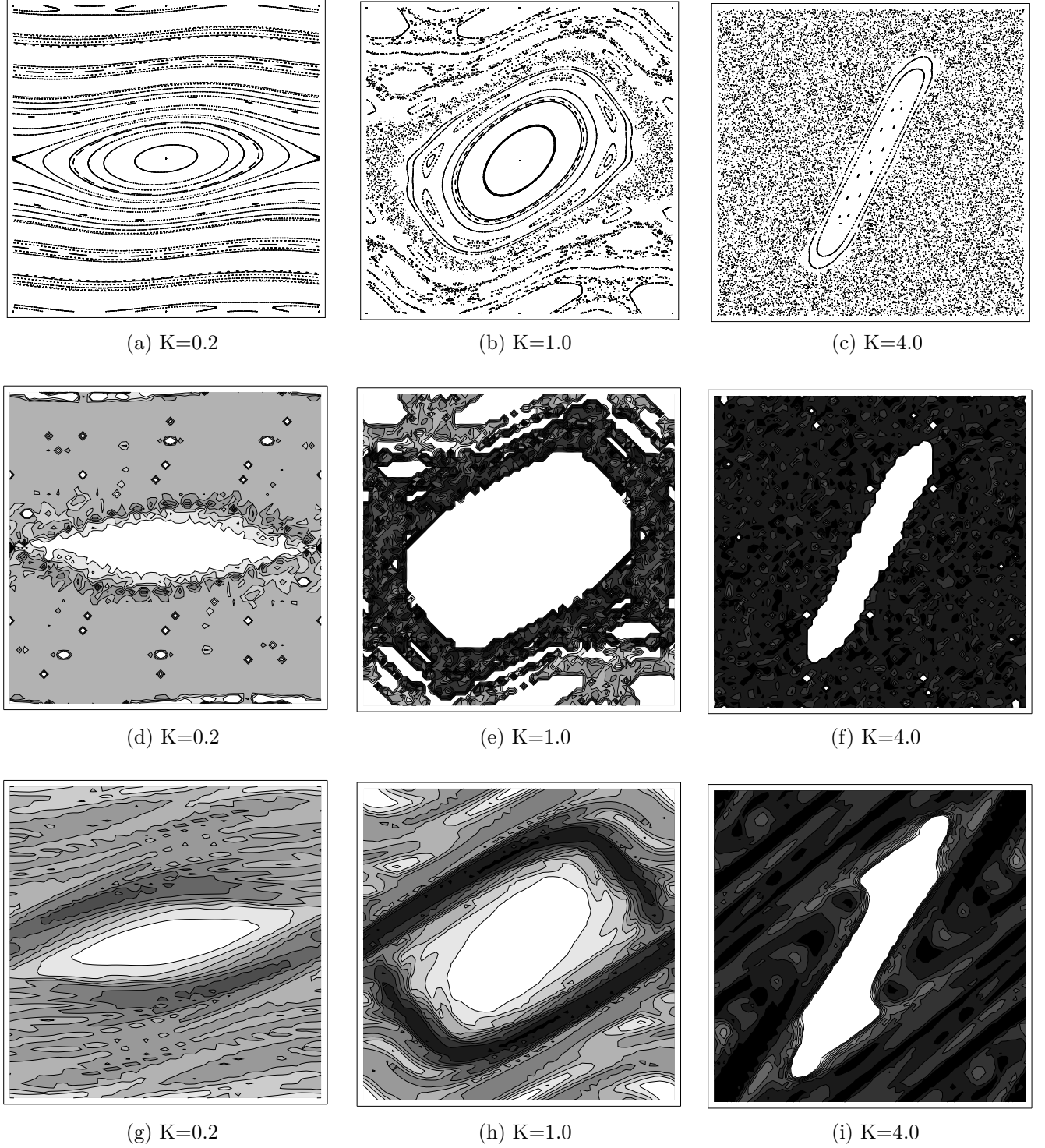


FIG. 1. Quantum-classical correspondence in the standard map. Three values of the chaos parameter K are shown for each set of maps clearly showing that correspondence is accurately maintained during the transition to global chaos. (a)-(c) Classical map in unit phase space bounded on the interval $[-\frac{1}{2}, \frac{1}{2}]$ for both q and p . (d)-(f) Contour plot of KS entropy in unit phase space for the classical map. (g)-(i) Contour plot of von Neumann entropy production rate in unit phase space for the quantum kicked rotor interacting with an environment.